

IoT System for Real-Time Near-Crash Detection for Automated Vehicle Testing

Ruimin Ke, Zhiyong Cui, Yanlong Chen, Meixin Zhu, Yinhai Wang

Abstract—Our world is moving towards the goal of fully autonomous driving at a fast pace. While the latest automated vehicles (AVs) can handle most real-world scenarios they encounter, a major bottleneck for turning fully autonomous driving into reality is the lack of sufficient corner case data for training and testing AVs. Near-crash data, as a widely used surrogate data for traffic safety research, can also serve the purpose of AV testing if properly collected. To this end, this paper proposes an Internet-of-Things (IoT) system for real-time near-crash data collection. The system has several cool features. First, it is a low-cost and standalone system that is backward-compatible with any existing vehicles. People can fix the system to their dashboards for near-crash data collection and collision warning without the approval or help of vehicle manufacturers. Second, we propose a new near-crash detection method that models the target’s size changes and relative motions with the bounding boxes generated by deep-learning-based object detection and tracking. This near-crash detection method is fast, accurate, and reliable; particularly, it is insensitive to camera parameters, thereby having an excellent transferability to different dashboard cameras. We have conducted comprehensive experiments with 100 videos locally processed at Jetson, as well as real-world tests on cars and buses. Besides collecting corner cases, it can also serve as a white-box platform for testing innovative algorithms and evaluating other AV products. The system contributes to the real-world testing of AVs and has great potential to be brought into large-scale deployment.

Index Terms—Automated vehicle, near-crash detection, corner case, Internet of Things, real-world testing, traffic video analytics

I. INTRODUCTION

NEAR-crash, or near-miss, has been a critical surrogate safety measure for transportation safety research [1]–[6]. The key reason is that the number of actual collisions in a certain scenario is often insufficient to support big data analytics or even traditional statistical models. Near-crashes are traffic incidents that have the potential to develop into collisions. They reflect the safety situations and designs, and are usually in much larger numbers than actual collisions. The most commonly used source for near-crash extraction is traffic surveillance video, given its low cost, wide deployment, and

rich information. The researchers at the University of British Columbia have been one of the leading groups dedicating to near-crash identification, extraction, and analysis using surveillance videos [7]–[10]. Recently, the City of Bellevue has been leading a collaborative effort with Microsoft and the University of Washington to develop large-scale video analytics for near-crash research using city-wide surveillance cameras in Bellevue toward the mission of Vision Zero [11].

With the emergence of automated vehicle (AV) concepts and technologies, near-crash becomes an even more valuable data source for not only traditional traffic safety research but also AV safety. The latest AVs have been demonstrated to be able to handle most situations they may encounter. However, the lack of corner cases for training and testing AVs is a major cause that is slowing down the pace to achieve the goal of Level-5 (L5) fully autonomous driving [12], [13]. The real corner case or collision data of AVs are rare due to at least two reasons: (1) the on-road testing scale of AVs is still very small, and (2) once there is a fatal accident, the test will likely to be suspended because of technical examination and public pressure.

While corner cases can be generated in simulations to support some AV research, it is a must step for future AVs to be tested with as many real-world corner cases as possible to ensure safety. The current on-road tests of AVs are mainly in the regions with plains and sunny weather, e.g., Arizona, California. In addition to the small testing scale, the lack of diversity in the testing scenarios is also a concern. In order to collect corner cases in any region or condition, it would be very helpful if we could have a system that can collect corner cases in any existing vehicles.

In this paper, we introduce an IoT system for real-time near-crash detection and data collection to support AV testing in the real world. The system is a low-cost and standalone system that is backward-compatible with existing vehicles. People can just fix the system to their dashboards for corner case collection, collision warning, and for AV algorithm innovation without the help or approval of the vehicle original equipment manufacturers (OEMs). The system is developed based on one of the latest IoT platforms, Nvidia Jetson TX2. The key method

This work was supported in part by the Safety Research and Demonstration (SRD) grant from the Federal Transit Administration (FTA) and in part by the Pacific Northwest Transportation Consortium (PacTrans).

Ruimin Ke, Zhiyong Cui, Meixin Zhu, and Yinhai Wang are with the Smart Transportation Applications and Research (STAR) Lab, Department of Civil and Environmental Engineering, University of Washington, Seattle, WA

98195, USA (e-mail: ker27@uw.edu, zhiyongc@uw.edu, meixin92@uw.edu, yinhai@uw.edu)

Yanlong Chen is with the Department of Mechanical Engineering, University of Tokyo, Bunkyo City, Tokyo, Japan (e-mail: chenyl@iis.u-tokyo.ac.jp).

in the system's main thread is a computer-vision-based near-crash detection method with real-time processing efficiency, high detection accuracy, and excellent transferability to any dashboard cameras. The near-crash detection method starts with understanding the motion patterns in the camera view, and then the selection of deep-learning-based object detection and online tracking. With the bounding boxes generated by the detection and tracking, we model the target road user's size changes and moving directions with linear-regression complexity to effectively estimate time-to-collision (TTC) and relative motions. Based on the TTC values and relative motions, we propose several new rules to near-crash identification. Moreover, we prove and show that our near-crash detection method is insensitive to intrinsic camera parameters, and this property makes it adaptable to any dashboard cameras. We design a few experiments to validate the system and demonstrate its great potential to accelerate AV innovation and research in multiple different ways.

The rest of the paper is organized as follows. In Section II, the authors conduct a thorough literature review on AV testing and summarize the related works from a new angle. In Section III, we introduce the proposed system in detail, including hardware components, software design, basis for the near-crash detection, detection framework and algorithms, and data collection functions. Section IV introduces the experiment designs and analysis, including the data description, experimental setup, evaluation metrics, parameter settings, completed tests, upcoming tests, and applications. We also create a YouTube video to present the near-crash detection.

II. RELATED WORK

In this section, we briefly review the related work in the field of AV testing. From the testing method perspective, existing studies can be divided into three categories: simulation-based testing, virtual-real testing, and real-world testing. The proposed IoT system contributes to the real-world testing area.

A. Simulation-Based Testing

Simulation for automated vehicle relies on the interactions between virtual agents and virtual environments to generate knowledge of the system or individual behaviors [14]. While there are quite a few widely used traffic simulation tools such as Synchro and VISSIM, none of them are designed exclusively for AV testing. Recently, introductions to the role of simulation in AV testing and exclusive simulators have been presented [15]. For example, Shah et al. designed AirSim as a high-fidelity AV simulation platform that offers physically and visually realistic simulations [16]. It allows algorithms developed on the simulator to be deployed to real vehicles without change, and it generates a large quantity of training data for building machine learning models. CARLA (Car Learning to Act) simulator was built from the ground up to support the development, training, and validation of AV systems [17]. It is an open-source platform and has generated significant influence in AV research. In addition to building AV simulation platforms, quite some studies focus on using simulation to validate new theories, models, and frameworks, targeting

accelerating AV testing and transferring them to virtual-real or real-world AV applications [18]–[25]. Zhao et al. conducted two pioneering studies on accelerating the evaluation of AV safety in lane-change and car-following scenarios [18], [19]. They first identified a significant number of lane-change and car-following events using naturalistic driving data and then modeled the behaviors using importance sampling techniques as the basis for scenario generation in simulation. Li et al. studied how to test the intelligence of AV and proposed a new testing approach that combined the benefit of scenario-based testing and functionality-based testing [20]. Their approach was applied to simulation testing in a parallel simulation platform. MIT researchers proposed a slot-based system to model AV traffic flow at intersections. They demonstrated in a simulation that the system had the potential to double the capacity of intersections [21]. Recently, Feng et al. published a two-part series of articles with a new theory in testing scenario library generation (TSLG) for AV [24], [25]. In part II of the study, three cases were investigated in simulation to demonstrate the superiority of their method.

B. Virtual-Real Testing

A key question for simulation-based AV testing is: how well does simulation match the real world? The answer varies from case to case, but no matter how well AV features and systems perform in simulation, it has to be tested in the real world at the end of the day. An intermediate step between simulation and real-world testing is the combination of them [26]–[34]. In some places, this type of virtual-real testing is called hardware-in-the-loop (HIL) testing. Researchers at the University of Michigan built an augmented reality (AR) environment that combined the VISSIM simulator and MCity test track [32]. The testing vehicles in the real world were synchronized with simulation. This pioneering virtual-real platform has been the support for more recent AV studies. For instance, Feng et al. took one step further by integrating their innovative TSLG theory [24], [25] into this platform to generate critical scenarios in the simulation and then interact with the real vehicles at the test track [26]. Similar research was led by UC Berkeley, in which they presented a formal method to generate test scenarios for AV in simulation and effectively select and implement tests on the road [28]. They also made quantitative and qualitative comparisons between the recorded data from the simulation and the test track for the same synthesized testing cases. Another virtual-real platform developed by Japanese researchers was an AR vehicle, which ran on the test track with three cameras and three big monitors [30]. When the driver was driving the real car on the real road, virtual traffic situations were shown on the three monitors in front of the driver. With this setup, driver performances in critical scenarios can be evaluated and reproduced without the risk of real collision. Tettamanti et al. designed a testing environment for AV testing with a Smart car and simulation [34]. Instead of using roadside unit (RSU) for data transmission and VISSIM as the simulation platform [32], in this study, the two-way message transmission was done via CAN communication, and the simulation was developed in SUMO. Li et al. applied the parallel vision techniques to

transfer the real-world sensing data in the normal daytime to virtual-world sensing data in less frequently encountered situations for testing [31]. Sometimes, virtual-real testing with real tracks or vehicles can still be costly, labor-intensive, and time-consuming to set up [28]. Xu et al. showed that it was feasible to build an inexpensive and safe HIL platform to test certain AV functions with scaled vehicles and roadways [29].

C. Real-World Testing

Real-world AV testing is expensive regarding both time and cost, but it is a must-step for any AV technology to be ready for production. While large-scale real-world tests are typically led by high-tech industrial companies or vehicle OEMs, the testing can often be interrupted by budget cuts during uncertain times or the pressure from the public after a fatal accident. Since L5 AVs are far from ready, many academic institutions have been actively contributing to real-world AV testing as well, especially on the topics of algorithm/system innovation [35]–[38], technology evaluation [39]–[41], field tests for traffic modeling [42], [43], field data generation [6], [44]–[46], etc. In the Stadtpilot project, Nothdurft et al. tested autonomous driving on Braunschweig’s inner-city ring road with a vehicle called Leonie [35]. Leonie was one of the very first worldwide to demonstrate the ability of self-driving vehicles. A few other projects have been conducted to test certain AV features designed by the team on open roads, such as the test of a sensor-independent fusion approach at Ulm University [37], the test of the BRAiVE prototype by VisLab including a trip from Itay to China [38], and the test in Parma urban roads and freeways [36]. Though these AV tests on open roads are not intended to be a demonstration that fully autonomous driving has been realized, the experience and findings are precious and are considered as a demonstration of the possibilities of L5 AV. The STAR Lab at the University of Washington has been collaborating with industrial partners and the government to conduct AV technology evaluation [39], [40]. In a TRB IDEA project, we evaluated the MobilEye Shield+ system on 38 buses in Washington State. We found that the system had the potential to reduce transit-related collisions as well as insurance costs [39]. This type of collaboration that involves academia, industry, and the government can accelerate AV testing by sharing the resources and expertise. In the sub-category of field tests for traffic modeling, tests on tracks or open roads with mixed traffic are designed to reveal the impact of AV to traffic and driver behaviors. Zhao et al. focused on the characteristics of mixed traffic and studied car-following behaviors of HV-following-AV and HV-following-HV with the position, velocity, and acceleration data [42]. Raboy et al. studied a field experiment on lane-change maneuvers, and their proposed testing platform could also be used to model and evaluate other research subcomponents of AV [43]. Data is the new oil and an essential foundation for AV functions. Another sub-category of research focuses on generating new data for benchmarking AV-related algorithms and approaches. For example, KITTI is a representative benchmark suite that provides a variety of sensing data for AV algorithms such as road detection, object detection, object tracking, depth estimation, optical flow

estimation, etc. [44]. It has generated a great influence on AV research. Other example studies such as vehicle-pedestrian near-miss data collection [6] and physical-world-resilient adversarial data generation [45] have been conducted as well.

III. IOT-BASED SOLUTION AND DESIGN

A. IoT System Hardware Components

The IoT system’s key components (see Figure 1) include an Nvidia Jetson TX2 device, a Logitech USB camera, a BU-353S4 USB GPS receiver, a Bestek DC-AC power converter, and a Honda car.

The Nvidia Jetson TX2 is configured with JetPack version 3.2.1; it preinstalls CUDA, OpenCV, etc. onto its operating system. But we recommend reinstalling the OpenCV for complete functionality. In this study, OpenCV 3.4.0 is reinstalled. Also, TensorFlow with the TensorRT support needs to be installed for object detection. TensorRT is an SDK that quantizes and optimizes TensorFlow graphs for high-performance deep learning inference. It is critical for IoT applications with Nvidia IoT devices.

The video input to the system is from a USB camera, which is mounted on the windshield facing front. The video quality and installation position are similar to those of a regular dashcam. Another system component that is connected to the IoT device is the GPS receiver. It is recognized as a serial port in Jetson’s Ubuntu 16.04 operating system. To invoke the GPS recording function, a Python library Pyserial needs to be installed. It enables reading GPS locations in real-time. The system’s power supply is from the car’s onboard cigarette lighter. A DC-AC converter is used to convert the DC power from the cigarette lighter to power the Jetson device. It also provides power to a monitor so that we can debug and modify codes and settings in the car when necessary.

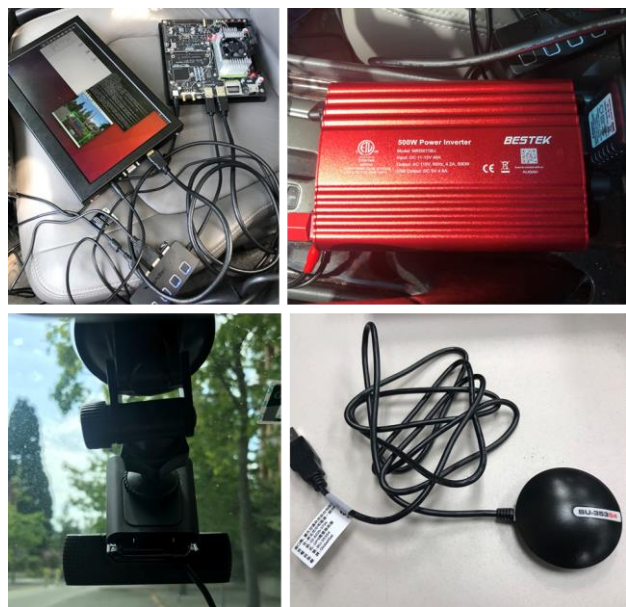


Fig.1 The key hardware components of the IoT system: Nvidia Jetson TX2 and a monitor (top left), Logitech USB camera (bottom left), Bestek DC-AC converter (top right), and the BU-353S4 GPS receiver (bottom right). These components are installed in a Honda car.

B. Understanding Relative Motion Patterns for Near-Crashes

Relative motions between the ego-vehicle and other road users are important cues for near-crash detection using a single camera [6], [47]. In order to design a good algorithm, it is necessary to understand the indications of certain relative motion patterns as well as the relationship between a pattern in the camera view and its corresponding pattern in the real world (see Figure 2). The relative motion patterns between two road users vary from case to case. Roadway geometry, road user's behavior, relative position, traffic scenario, etc. are all factors that may affect the relative motion patterns. For example, from the ego-vehicle's perspective, its relative motion to a vehicle that it is overtaking in the neighbor lane and that to another vehicle it is following in the same lane are undoubtedly different.

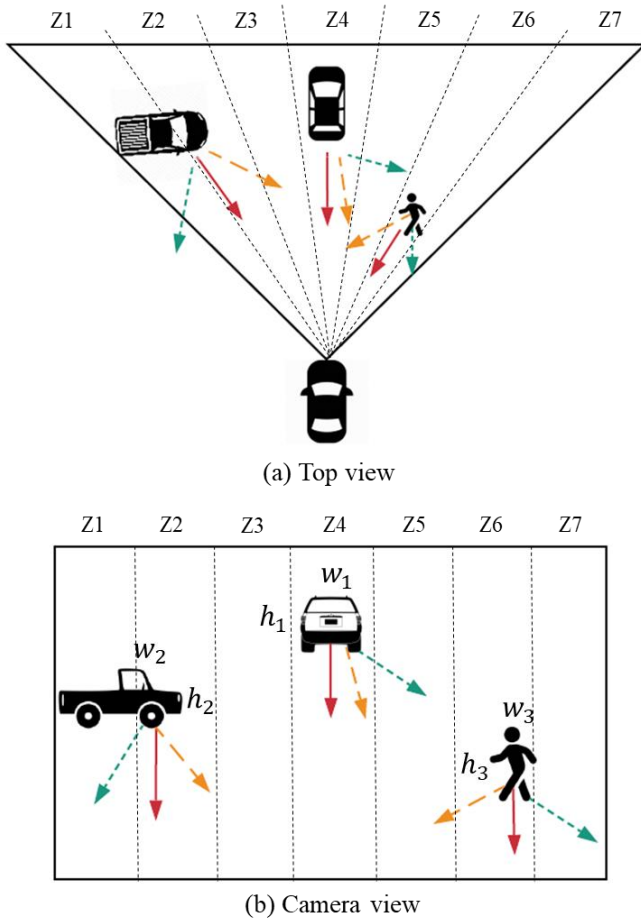


Fig. 2 The corresponding relative motions, relative locations, and lines of sights between the ego-vehicle and three other target road users. In the case of target's size increasing in the camera view, there are still three types of relative motions between the ego-vehicle and the target road user — solid red arrows: potential crashes; dotted yellow arrows: warnings; dotted green arrows: safety.

Despite a large number of different patterns, a relative motion that has the potential to develop into a crash / near-crash has a property in common: From the ego-vehicle's perspective, the target road user would be moving towards it. Because of camera properties, this kind of relative motion for a potential

crash is shown as a motion vector of the target road user moving vertically towards the bottom side of the camera view. Examples are shown as solid red arrows in Figure 2. In the real-world top view, the three solid red arrows represent the relative motions between the ego-vehicle and three other road users (a pick-up truck, a car, and a pedestrian). Each of the three relative motion vectors aligns with a line of sight of the camera (Z2, Z4, and Z7). In the camera view, the lines of sight are shown as vertical bands. The relative motion vectors for near-crashes in the top view correspond to vectors moving towards the bottom in the camera view aligning with Z2, Z4, and Z7.

Two road users have a relative motion at any time. In addition to the case of a near-crash defined above, it is worth introducing other patterns. First of all, a target road user may move towards the ego-vehicle, move away from the ego-vehicle, or stay at the same distance to the ego-vehicle. They can be identified as size changes in the camera. This property will be utilized later in our approach. Either size decreasing or no size change would not lead to crashes / near-crashes. For size increasing, there are still three different cases. The first case is the potential crash case, shown as the solid red arrows in Figure 2. The second case is the warning case, shown as the dotted orange arrows. It means the relative motion is towards the center line of sight of the camera (the pick-up truck and the pedestrian), or the relative motion is just slightly different from the solid red arrow while the target road user is at the center line of sights (the car). The warning case could still develop into crashes if there are slight changes in the speeds or headings of either the target or the ego-vehicle. The third case is the safety case that relative motion is moving away from the center line of sights, shown as the dotted green arrows in Figure 2.

C. Software Flow Diagram

The flow diagram of the overall software design is shown in Figure 3. The two major functions of the system are near-crash detection and data collection. Given the real-time operation requirement for both functions, the design should be simple enough to support this need for high efficiency and sophisticated enough to make good use of the IoT device's computational power for high accuracy and reliability. Besides, it would be desirable if the near-crash detection method could be insensitive to different camera parameters so that future large-scale deployment would be accelerated.

The software is implemented in a multi-thread manner. Three different threads are operating simultaneously: the main thread, the data collection thread, and the video frame reading thread. The proposed near-crash detection method is implemented in the main thread. When near-crash events are detected, a trigger will be sent to the data collection thread, and it will record video frames from a queue (a global variable) and other data that are associated with the near-crash event. The third thread for video frame reading keeps the latest video frame that the camera captures in another queue; it will dump previous frames when the capturing speed is faster than the main thread's frame processing speed.

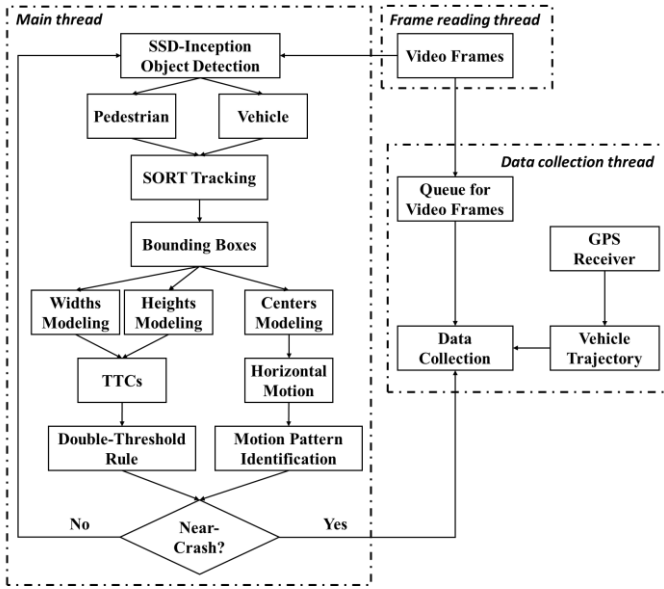


Fig. 3 The software flow diagram for the IoT system

D. Real-Time Camera-Parameter-Free Near-Crash Detection

In this sub-section, we introduce the design and development of the near-crash detection method in detail.

1) Deep-learning-based road user detection and tracking

The main thread starts with applying a deep-learning-based object detector to every video frame. Deep-learning-based object detection can simultaneously localize and classify objects with high accuracy [48], [49]. It has become a standard feature of the latest AV technologies. However, one disadvantage of deep-learning-based inference is its high computational cost, which prevents it from being deployed for certain applications. As one of the most powerful IoT devices at present, Nvidia Jetson TX2 is capable of running some deep object detectors in real-time and running the inference with TensorRT-optimized inference neural networks.

For traditional IoT devices, Tiny Yolo and SSD-MobileNet are two of the most popular deep-learning-based detectors given their high inference efficiency. But we find that a more complicated detector, SSD-Inception, is also a real-time detector on Jetson TX2 with nearly 30 frames-per-second (FPS) detection speed and much better accuracy. Therefore, we choose SSD-Inception as the object detector for our system. The system keeps detected pedestrians and vehicles for further processing.

The object detection gives out bounding boxes and the types of road users in every individual video frames. In order to associate the information from the different frames and find each road user’s movement, a standard step following object detection is object tracking. SORT tracking is a recent benchmark for object tracking with online and real-time performance. It achieves good tracking accuracy without the need for any complicated features but solely the bounding box information. It also can get rid of some false-positives and false-negatives that are generated in the detection phase. Some studies demonstrate it to be a suitable tracking method for intelligent transportation applications [50], [51].

2) Modeling bounding boxes in linear-regression complexity for camera-parameter-free TTC estimation

Intuitively, an object appears larger in the camera view as it is approaching the camera, and vice versa. Researchers at MobilEye published a paper as early as in 2004 to show that it was possible to determine TTC using size changes [52]. In this study, the proposed approach for TTC estimation mainly considers: (1) leveraging the power of recent achievements in deep learning, (2) making the computation as efficient as possible to support real-time processing on Jetson, and (3) transferrable to any dashboard camera without knowing the camera’s intrinsic parameters.

The first consideration of utilizing deep learning has been realized and introduced in the last sub-section. SSD+SORT detects and tracks road users with high accuracy. However, the next step, which is the near-crash identification, has to be very simple and effective. Otherwise, the real-time requirement would not be satisfied with the IoT device.

The object detection and tracking provide not only the location and category of objects but also their sizes with the bounding boxes information. However, bounding boxes are just approximate sizes of the objects and are not supposed to be used for accurate determination of objects’ sizes. Particularly, given two consecutive frames, the size change of an object is subtle; and in many cases, this change is not recognizable given the noises in the bounding boxes generation. We are calling it “noises” rather than “errors” here because, as just mentioned, bounding boxes generated by an object detector are not supposed to determine the exact size of an object. In our initial experiment, we also found that the size of an object in the previous frame may be even larger than that in the next frame.

In addition to the “noises” thing, another reason for the inaccurate size change detection in neighboring frames is that the time is too short in between two consecutive frames. Given a video with a frame rate of 24 FPS, the next frame is captured in less than 0.05 seconds. Thus, we came up with an idea for size change detection: (1) to use more frames to compensate for the noises in every single frame, (2) to increase the time interval for the detection. This idea leads to the solution of using linear regression for either the bounding boxes’ heights or widths over a group of consecutive frames. And we found that the best number of sizes (or frames) for regression is about 10 to 15. This is reasonable given that (1) the number of 10 to 15 frames are large enough to compensate the noises, (2) the time associated with 10 to 15 frames is still small enough (about half seconds) to assume that the road user’s motion is consistent.

So, the input to the linear regression is a list of heights or widths extracted from the bounding boxes, and the slope outputted by the regression will be the size change rate. Let us denote the size change rate as r_t , and the size of the road user in the video frame as s_t at time t . At the same time, in the real world, the longitudinal distance between the target road user and the ego-vehicle is D_t , the relative longitudinal speed is V_t , the target road user’s size is S_t , and the camera focal length is f . Based on the pinhole camera model, there is

$$\frac{s_t}{f} = \frac{S_t}{D_t} \quad (1)$$

We also know that relative speed is the first derivative of relative distance, and that size change rate is the first derivative of the object size over time

$$V_t = \frac{dD_t}{dt}, \quad r_t = \frac{ds_t}{dt} \quad (2)$$

Since the real-world target road user's size does not change over time, there is the following equation

$$0 = \frac{dS_t}{dt} = \frac{d\left(\frac{D_t S_t}{f}\right)}{dt} \quad (3)$$

And since the focal length does not change over time, we have

$$0 = \frac{d(D_t S_t)}{dt} = \frac{dD_t}{dt} \cdot s_t + \frac{ds_t}{dt} \cdot D_t = V_t s_t + r_t D_t \quad (4)$$

Thus,

$$TTC = -\frac{D_t}{V_t} = \frac{S_t}{r_t} \quad (5)$$

According to Eq. (5), TTC can be calculated as the size of the bounding box at time t divided by the size change rate at time t . It is not related to the focal length or other intrinsic camera parameters. The TTC value can be either positive or negative, where being positive means the target is approaching the ego-vehicle, and being negative means it is moving away from the ego-vehicle.

3) Height or width?

There are two options for the size of the road user in the camera view, height and width. We argue that height is a better indicator than width. From the ego-vehicle's perspective, it may observe a target vehicle's rear view, front view, side view, or a combination of them, depending on the angle between the two vehicles. That is to say, the bounding box's width change may be caused by either the relative distance change or the view angle change. For example, when the ego-vehicle is overtaking the target vehicle, or the target vehicle is making a turn, the view angle changes and will lead to the bounding box's width change.

However, the bounding box's height of the target vehicle is not influenced by the view angle; it is solely determined by the relative distance between the two vehicles. Similarly, a pedestrian walking or standing on the street may have different bounding boxes' widths due to not only the relative distance to the ego-vehicle but also the pose of the pedestrian; but the height of a pedestrian is relatively constant.

Despite the challenge of using width to determine an accurate TTC, it still provides valuable information. Since we are using only less than one second of frames for the calculation, the view change does not contribute as much as the distance change, so

width still roughly shows the longitudinal movement of the road user. This is very important in some cases. For instance, a vehicle moving in the opposite direction of the ego-vehicle is truncated by the video frame boundary. In this case, the height of the vehicle increases while the width decreases. This is not a near-crash case at all, but the TTC can be very small and falsely indicate a near-crash by only looking at the height change.

We propose a double-threshold rule: if the TTC threshold for determining a near-crash is δ , we will set this δ as the TTC threshold associated with the height regression. At the same time, we have another TTC threshold φ associated with the width regression. The second threshold φ is to ensure that the width and height changes are in the same direction. The rule is represented as

$$0 < \frac{h}{r_h} < \delta, \quad 0 < \frac{w}{r_w} < \varphi, \quad \delta < \varphi \quad (6)$$

where r_h and r_w are the change rates for height h and width w . It is a necessary condition for a near-crash.

4) Modeling bounding box centers for horizontal motion pattern identification

As shown in Figure 2, there are three scenarios for the case that a road user approaches the ego-vehicle; they correspond to potential crashes, warnings, and safe scenarios. Besides TTC, these scenarios can be differentiated with the relative horizontal motion between the ego-vehicle and the target. This needs to be calculated with computationally cheap methods as well. We propose to apply another linear regression using a list of bounding box's centers of the target road user. The regression result would be able to indicate the moving direction of the road user in the camera view.

In general, when the target's location is closer to the bottom and closer to the center line of sight, the risk of a collision is higher, so the threshold for the moving direction ω is looser. We propose a rule to show this judgment as

$$\alpha < \omega \cdot (C_x - C_{los}) \cdot (B_y - B) < \beta \quad (7)$$

where C_x is the center's x coordinate, C_{los} is the center line of sight, B_y is the bottom side of the bounding box, and B is the bottom of the video frame. Since cameras have different resolutions, $(C_x - C_{los})$ is normalized to $[-1, 1]$ and $(B_y - B)$ is normalized to $[0, 1]$. The two thresholds are α and β ; α should be set to negative to capture the potential warning scenarios (the orange dotted arrows in Figure 2). And β should be just slightly larger than zero to capture the potential crashes (the solid red arrows in Figure 2) and filter out most of the safe scenarios (the green dotted arrows in Figure 2). Eq. (6) and Eq. (7) together identify near-crash events.

E. Near-Crash and Vehicle Trajectory Data Collection

The near-crash events and related data are collected in a separate thread when receiving triggers from the main thread. In this paper, the trigger is solely sent by the main thread when near-crashes are detected using the proposed approach. It is

possible to add other types of triggers to the system. The next version of this system will include the integration of a LiDAR-based technology for collision avoidance and automated braking, so the system will have a function to identify and process different triggers.

In this study, the system collects video clips data (from 10 seconds before the near-crash and 10 seconds after the near-crash), event type data, TTC-height data, TTC-width data, event's time, and event's GPS location. At the same time, the system constantly collects vehicle trajectory data with the GPS receiver every three seconds. The frequency can be adjusted in the program for different purposes and requirements.

IV. EXPERIMENTAL RESULTS AND ANALYSIS

A. Experiment Design

Local experiment with locally stored videos at Jetson and real-world experiment with onboard real-time video feeds were selected as two groups for testing the system. Local video resources were abundant that covered a lot of historical near-crash scenarios as well as other corner cases. It was a better source to evaluate the near-crash detection method we proposed in this paper. Real-time video data was captured by the system in real-time while driving a vehicle. This was a necessary step to test the system's performance in the real world, which helped evaluate not only the software but also the engineering details.

Over 100 hours of tests have been conducted so far. The local video data were collected from online platforms (e.g., YouTube) and some team members' dashboard cameras (see Figure 4 for some examples). Real-world tests have been conducted on two Honda cars and two Pierce Transit buses. Most real-world tests were on the cars, while on-road tests on the buses are scheduled in the near future.



Fig. 4 Video data samples for the local tests on Jetson.

B. Parameter Settings

There were several key parameters needed to be set properly: SSD detector's confidence threshold, the number of frames for size regression, the number of frames for center regression, TTC threshold δ , TTC threshold φ , horizontal motion threshold α , horizontal motion threshold β , and Jetson's power mode. Given the fact that (1) SSD detector tended to have fewer false-positives than false-negatives [50], (2) some false-positives can be filtered out at the tracking step, and (3) more false-positives (if any) will be filtered out by the near-crash detection algorithm, we set the detection confidence threshold relatively small to be around 0.3 – 0.5.

For the number of frames for size regression, we suggested

setting them to be around 10 to 15 frames. This range was large enough to compensate for the bounding box noises and small enough to assume the target's motion is consistent. The number of frames for center regression can be a little larger to capture the horizontal motion better, and the suggested number was in the range of 15 to 20. For δ and φ , as defined by many previous studies, the TTC threshold for a near-crash was around 2 to 3 seconds, which was our suggested value for δ . And we found that setting φ to about 2 to 2.5 times of δ worked well. We suggested setting α to the range of [-1, -0.5] and β to [0.02, 0.1]. Jetson's power mode was recommended to be set as Max-N to fully utilize its computational power, though our system still operated in real-time (but lower FPS) with Max-Q mode.

C. Experiment with Local Video Feeds

1) Evaluation design

Experiment with local video feeds is running the system with locally stored videos on Jetson. Essentially, near-crash is a type of traffic anomaly. So, to evaluate the proposed method's accuracy, we used the evaluation process of the Traffic Anomaly Detection task (Track 4) of the 2020 AI City Challenge as the reference [53]. First, the task dataset has 100 video clips with some anomalies. It is unknown exactly how many anomalies are in the test dataset, but the number is between 0 and 100, as mentioned in the introduction to Track 4. Likewise, we made a local test dataset with 100 video clips (Figure 4) and 35 near-crash events. As aforementioned, the test videos were from online resources and private cars' dashboard cameras; therefore, we are not going to publish this dataset considering potential privacy and copyright issues. However, the authors do have a desire to create such a video dataset for near-crash detection in the future.

We manually labeled all the near-crash events regarding their occurrence videos and times. Like in AI City Challenge Track 4, we defined a true-positive (TP) as a predicted near-crash within 10 seconds of the true near-crash. A false-positive (FP) is a predicted near-crash that is not a TP for some near-crash. A false-negative (FN) was a true near-crash that was not predicted. We used the F1 score to evaluate accuracy. F1 score was the harmonic mean of the precision and recall

$$F1 = 2 \cdot \frac{\text{precision} \cdot \text{recall}}{\text{precision} + \text{recall}} = \frac{2TP}{2TP + FP + FN} \quad (8)$$

where its best value at 1 and the worst value at 0.

2) Evaluation results

Some sample near-crash detection results are shown in Figure 5. The top three rows were three vehicle-vehicle near-crashes, and the bottom two rows were two of the vehicle-pedestrian near-crashes. The bounding boxes would become red as the indicator of a predicted near-crash, while all the other detected road users were with green bounding boxes. More sample detection results can be found at the video we published on YouTube (the link is in the caption of Figure 5).

As summarized in Table I, our system correctly predicted 34 out of the 35 labeled near-crashes and missed 1 of them. Besides, it generated 7 FPs in the 100 video clips. Based on Eq. (8), the

final F1 score was 0.895, and the average processing speed with Max-N mode was about 18 FPS. The performance was promising, considering that we intentionally included a variety of near-crashes and some very challenging scenarios in the dataset. There were adverse weather conditions, nighttime situations, traffic congestion, urban/rural traffic scenes, etc.

Table I Evaluation results

# of videos	# of events	TP	FP	FN	F1 Score	FPS
100	35	34	7	1	0.895	18

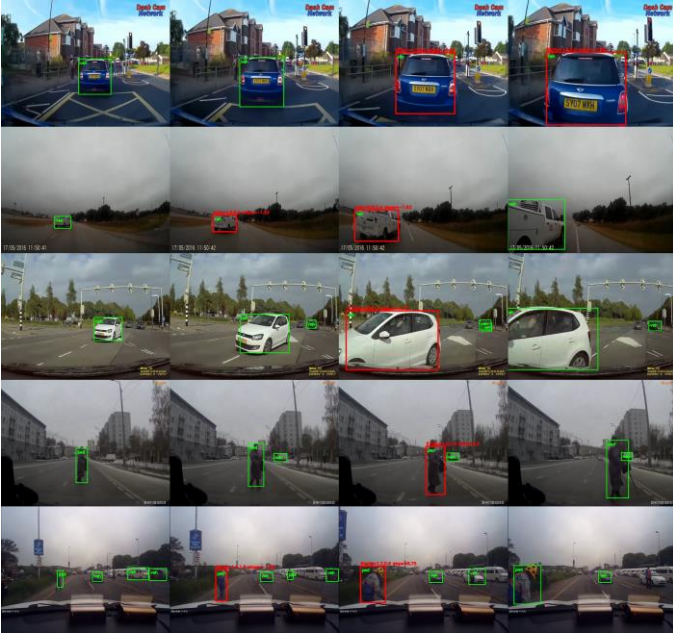


Fig. 5 Sample detection results with the local video experiment. Each row is a four-frame sub-sequence of one near-crash. More detection results can be found at the demo video we made (link: <https://www.youtube.com/watch?v=8qu-cNqfWkg>).

It is worth mentioning that our system knew nothing about the camera parameters of any of these nearly 100 cameras (some video clips were recorded by the same camera). This impressive result benefited from the proposed near-crash detection method. It again highlighted the possibility of applying the IoT system in a large scale for AV corner case collection with low cost and high efficiency.

We carefully examined the FN and FP cases and summarized the causes of them. The only FN was that the system missed a vehicle-pedestrian near-crash at night on a rural freeway with no streetlight. The pedestrian violated traffic rules by crossing the freeway, and the driver did not see him until almost running into him. The pedestrian was entirely in the dark so that the object detector missed him. Though there were more FPs than FNs, we considered having only seven FPs was acceptable and encouraging given the tradeoff in the efficiency of the system. While the proposed near-crash detection method can compensate for the bounding box size noises in most cases, it was still not perfect. In the fourth case (the fourth row) of Figure 5, right before the correct detection of this vehicle-pedestrian near-crash, there was a vehicle-vehicle FP caused by the significant error in the vehicle size detection. It was included in

our YouTube demo video. To further improve the detection performance, a practical solution is to improve the object detector by transfer learning with more data.

D. Real-World Experiment

The real-world experiment was conducted to test the real-time operation, data collection, and system reliability. So far, most real-world tests were done the two Honda cars in Seattle, WA. Note that we have also done some initial tests of the system on two Pierce Transit buses in Tacoma, WA. The experiment in the real world was more challenging than in the lab, even for the same system. We noticed a few things that were worth being summarized.

While in the local test, Jetson processed the local videos frame by frame; in the real-world test, different camera hardware, settings, or different software design resulted in different frame-reading speed and stability. This was why we had a separate thread for video capture to ensure the frame captured by the system was the latest.

Also, when doing the regressions for near-crash detection, the system got to include the corresponding time for each value (height, width, and center) in the regression because the interval between every pair of neighboring frames may not be uniformly distributed.

Moreover, the camera type may influence the system's performance. We noticed the video captured on the bus had about 2-3 seconds of latency, while on the car, there was no observable latency. This was a hardware issue that the video feed on the bus was from an IP camera connected via ethernet cables to the IoT system.

We also observed that the GPS coordinates collected by the GPS receiver were not in any of the standard formats. We spent quite some time to figure out there was a linear relationship between the raw GPS coordinate and the WGS84 coordinate format. The conversion is shown as follows in Eq. (9) and we hope this information will be helpful to whoever is going to use the same GPS receiver for their projects.

$$\begin{cases} Lat_{WGS84} = 1.666 \times Lat_{raw} - 31.30174 \\ Lon_{WGS84} = 1.666 \times Lon_{raw} + 81.25186 \end{cases} \quad (9)$$

Figures 6 and 7 presented a sample of event data and GPS data we collected in the real-world experiment. Figure 6 included three near-crashes around the University of Washington (UW) campus. The first one was on campus with a car, and the second one was on the 15th st. in the University District with a King County Metro bus, and the last one was at the west of campus near University Village. All the data associated with these events, including the event video clips, the TTC values, the event types, the GPS locations, and the occurrence times, were successfully recorded. Note that we were also able to calculate the vehicle speeds using the GPS data. Figure 7 showed the trajectories and two near-crash events' spots on the OpenStreet Map with the corrected GPS coordinates during a trip on the UW campus. The GPS trajectory and event location data are valuable sources for analyses such as hotspot mapping and clustering.

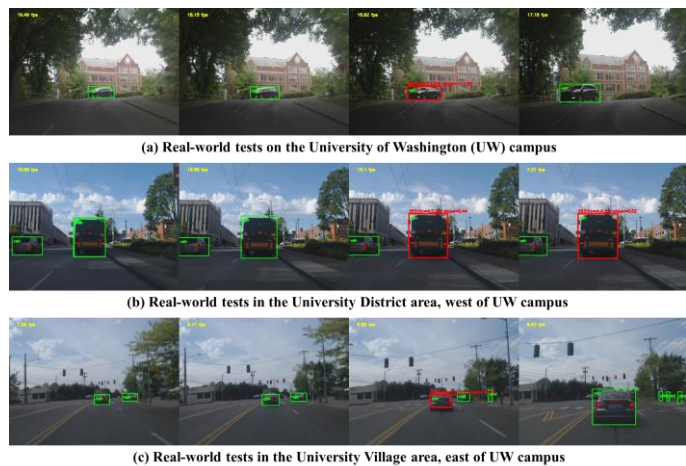


Fig. 6 Three sample near-crashes captured around the UW area in the real-world experiment: a) on campus, b) west of campus, c) east of campus. The last two clips in our demo video show a vehicle-vehicle event detected in the car and another vehicle-pedestrian event detected on the bus (link: <https://www.youtube.com/watch?v=8qu-cNqfWkg>). These last two video clips were taken by phone to better demonstrate the real-time operation of the system.

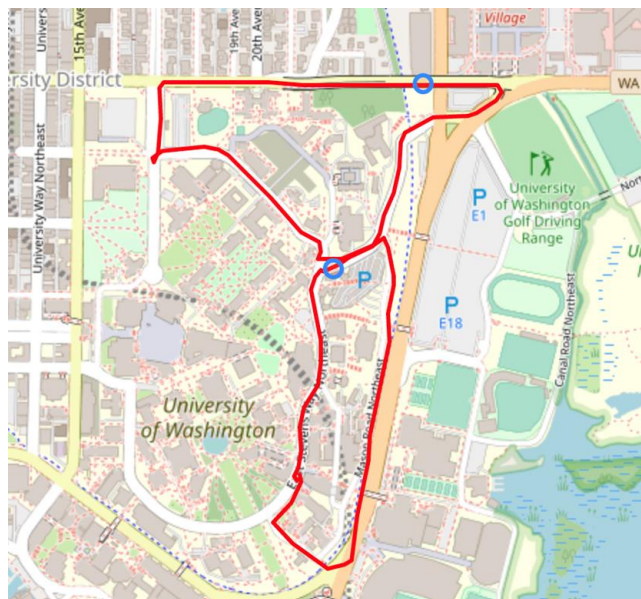


Fig. 7 Sample GPS trajectory data (the red curves) and two near-crash events (the blue circles) collected by the system during a trip.

E. Upcoming On-Road Test on Pierce Transit Buses

The development of the system is sponsored by a Federal Transit Administration (FTA) project led by Pierce Transit, the upcoming tasks include the integration and on-road testing of several systems. Our system will be installed on four Pierce Transit buses and integrated with the Pedestrian Avoidance Safety System (PASS) that uses LiDAR to trigger automated deceleration and braking. A few more components will be delivered on our end on top of the system functions introduced in this paper.

First, there will be a communication module. Our system will exchange messages with the PASS system via CAN bus. The CAN communication is developed with the Peak-CAN adapter and the SocketCAN Python library. Second, instead of

recording the data locally at Jetson, all the data will be transmitted to a server in real-time. Hence, we have been developing and testing a data transmission module on Jetson to make sure the transmission of videos and other data is fast and reliable. Third, Jetson TX2 does not support auto boot-up. It will be a problem if the system needs someone to manually push its power button every time the bus starts up. Thus, our team has developed an external circuit driven by Arduino Nano to automatically boot up the system when the bus power is on. Figure 8 is a picture of our system being installed in the bus cabinet of Pierce Transit bus #230, and being tested for individual functions.

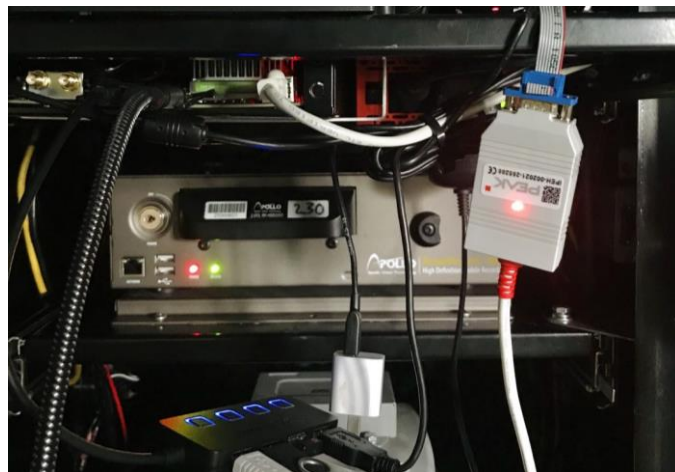


Fig. 8 The IoT system being tested on a Pierce Transit bus.

F. Applications to Automated Vehicle Research

The proposed system and the design idea behind it have a broad application and potential to benefit and accelerate AV research in multiple ways.

1) *A cost-effective corner case collection tool to enhance AV safety:* One of the biggest gaps between L5 autonomous driving and state of the art in AV technology is that there are insufficient corner case data for training and testing AVs to handle every possible situation in the real-world appropriately. The proposed system has the advantages of being cost-effective, easy for installation, well-performed in detection, and compatible with various dashboard cameras. There are nearly 300 million registered vehicles just in the United States. Imagine installing such a system on even only a small portion of the existing vehicles for corner case collection, and how valuable the data would be for us to move one step closer to L5 autonomous driving?

2) *A standalone system for real-world testing of AV features:* One of the major tasks in the FTA project is to use this system as a real-time event logging unit and smart data hub for the evaluation of the PASS autonomous driving technology. As a standalone system with detection and communication capabilities, it can be used for evaluating a variety of AV features. In a previous project to evaluate the MobilEye Shield+ system [39], we spent a lot of time and hard drive space to store and process all the videos collected on 38 buses in three months. But in this FTA project, with the help of this system, we are able to filter out most of the videos with no interested events in

real-time to make the post-evaluation much more efficient.

3) *A backward-compatible platform for accelerating innovation of new ideas in AV research*: The authors consider the way we build and test the proposed system can be a useful reference for the community. Essentially, the system is a backward-compatible platform for existing vehicles that allows customized designs of hardware and software. Anyone who has any new idea, either an algorithm or a function, regarding AV perception, planning, prediction, control, etc. can probably test his or her idea in a relatively short time with relatively low cost on any existing vehicle. This will surely accelerate innovations for AV research. We also showcase an example of how to design suitable methods with high efficiency and reliability on IoT devices for AV research.

V. CONCLUSION

In this paper, we introduced the design, development, and evaluation of an IoT system for real-time near-crash detection for the purpose of automated vehicle testing. We did a thorough literature review on automated vehicle testing methods. The proposed system was backward-compatible with any existing vehicles so that the installation could be very convenient. The system's design, detection framework, proposed algorithms, near-crash identification rules, and parameter settings were described in detail. The proposed near-crash detection method was fast, accurate, reliable, and insensitive to camera parameters by modeling the bounding boxes that were generated by object detection and tracking in linear-regression complexity. These features made the system adaptable to different vehicles' dashboards and showed the possibility for large-scale deployment. The experiments consisted of local tests at Jetson with 100 video clips and real-world tests on cars and buses. The experimental results were promising. The proposed IoT system was among the first efforts to collect near-crash data in a real-time manner to support addressing a key bottleneck in realizing fully autonomous driving. We also introduced our upcoming on-road tests on Pierce Transit buses and example applications of the system to accelerate AV research.

ACKNOWLEDGMENT

The authors would like to thank FTA and PacTrans for funding this research. We also express gratitude to our research partners (Pierce Transit, WSTIP, DCS Inc., VTTI, Volpe Lab, CUTR, Veritas, Dr. Jerome Lutin, Janet Gates, etc.) in the FTA project team for their invaluable contributions and suggestions.

REFERENCES

- [1] S. G. Klauer, T. A. Dingus, V. L. Neale, J. D. Sudweeks, D. J. Ramsey, and others, "The impact of driver inattention on near-crash/crash risk: An analysis using the 100-car naturalistic driving study data," 2006.
- [2] J. Wu, H. Xu, Y. Zheng, and Z. Tian, "A novel method of vehicle-pedestrian near-crash identification with roadside LiDAR data," *Accid. Anal. Prev.*, vol. 121, pp. 238–249, 2018.
- [3] A. Talebpour, H. S. Mahmassani, F. Mete, and S. H. Hamdar, "Near-Crash Identification in a Connected Vehicle Environment," *Transp. Res. Rec.*, vol. 2424, no. 1, pp. 20–28, 2014.
- [4] H. Makizako *et al.*, "Associations of near-miss traffic incidents with attention and executive function among older Japanese drivers," *Gerontology*, vol. 64, pp. 495–502, 2018.
- [5] H. Kataoka, T. Suzuki, S. Oikawa, Y. Matsui, and Y. Satoh, "Drive video analysis for the detection of traffic near-miss incidents," in *2018 IEEE International Conference on Robotics and Automation (ICRA)*, 2018, pp. 1–8.
- [6] R. Ke, J. Lutin, J. Spears, and Y. Wang, "A Cost-Effective Framework for Automated Vehicle-Pedestrian Near-Miss Detection Through Onboard Monocular Vision," in *IEEE Computer Society Conference on Computer Vision and Pattern Recognition Workshops*, 2017, vol. 2017-July.
- [7] T. Sayed, M. H. Zaki, and J. Autey, "Automated safety diagnosis of vehicle-bicycle interactions using computer vision analysis," *Saf. Sci.*, vol. 59, pp. 163–172, 2013.
- [8] K. Ismail, T. Sayed, N. Saunier, and C. Lim, "Automated analysis of pedestrian-vehicle conflicts using video data," *Transp. Res. Rec.*, vol. 2140, no. 1, pp. 44–54, 2009.
- [9] K. Ismail, T. Sayed, and N. Saunier, "Automated analysis of pedestrian-vehicle conflicts: Context for before-and-after studies," *Transp. Res. Rec.*, vol. 2198, no. 1, pp. 52–64, 2010.
- [10] N. Saunier, T. Sayed, and K. Ismail, "Large-Scale Automated Analysis of Vehicle Interactions and Collisions," *Transp. Res. Rec.*, vol. 2147, no. 1, pp. 42–50, 2010.
- [11] F. Loewenherz, V. Bahl, and Y. Wang, "Video analytics towards vision zero," *Inst. Transp. Eng. ITE J.*, vol. 87, no. 3, p. 25, 2017.
- [12] J. Bolte, A. Bar, D. Lipinski, and T. Fingscheidt, "Towards Corner Case Detection for Autonomous Driving," in *2019 IEEE Intelligent Vehicles Symposium (IV)*, 2019, pp. 438–445.
- [13] G. Chou, Y. E. Sahin, L. Yang, K. J. Rutledge, P. Nilsson, and N. Ozay, "Using control synthesis to generate corner cases: A case study on autonomous driving," *IEEE Trans. Comput. Des. Integr. Circuits Syst.*, vol. 37, no. 11, pp. 2906–2917, 2018.
- [14] E. Thorn, S. Kimmel, and M. Chaka, "A Framework for Automated Driving System Testable Cases and Scenarios," 2018.
- [15] H.-P. Schöner, "Simulation in development and testing of autonomous vehicles," in *18. Internationales Stuttgarter Symposium*, 2018, pp. 1083–1095.
- [16] S. Shah, D. Dey, C. Lovett, and A. Kapoor, "Airsim: High-fidelity visual and physical simulation for autonomous vehicles," in *Field and service robotics*, 2018, pp. 621–635.
- [17] A. Dosovitskiy, G. Ros, F. Codevilla, A. Lopez, and V. Koltun, "CARLA: An open urban driving simulator," *arXiv Prepr. arXiv:1711.03938*, 2017.
- [18] D. Zhao *et al.*, "Accelerated evaluation of automated vehicles safety in lane-change scenarios based on importance sampling techniques," *IEEE Trans. Intell. Transp. Syst.*, vol. 18, no. 3, pp. 595–607, 2016.
- [19] D. Zhao, X. Huang, H. Peng, H. Lam, and D. J. LeBlanc, "Accelerated evaluation of automated vehicles in car-following maneuvers," *IEEE Trans. Intell. Transp. Syst.*, vol. 19, no. 3, pp. 733–744, 2017.
- [20] L. Li, W.-L. Huang, Y. Liu, N.-N. Zheng, and F.-Y. Wang, "Intelligence testing for autonomous vehicles: A new approach," *IEEE Trans. Intell. Veh.*, vol. 1, no. 2, pp. 158–166, 2016.
- [21] R. Tachet *et al.*, "Revisiting street intersections using slot-based systems," *PLoS One*, vol. 11, no. 3, p. e0149607, 2016.
- [22] M. Althoff and S. Lutz, "Automatic generation of safety-critical test scenarios for collision avoidance of road vehicles," in *2018 IEEE Intelligent Vehicles Symposium (IV)*, 2018, pp. 1326–1333.
- [23] G. E. Mullins, P. G. Stankiewicz, R. C. Hawthorne, and S. K. Gupta, "Adaptive generation of challenging scenarios for testing and evaluation of autonomous vehicles," *J. Syst. Softw.*, vol. 137, pp. 197–215, 2018.
- [24] S. Feng, Y. Feng, C. Yu, Y. Zhang, and H. X. Liu, "Testing scenario library generation for connected and automated vehicles, part I: Methodology," *IEEE Trans. Intell. Transp. Syst.*, 2020.
- [25] S. Feng, Y. Feng, H. Sun, S. Bao, Y. Zhang, and H. X. Liu, "Testing scenario library generation for connected and automated vehicles, part II: Case studies," *IEEE Trans. Intell. Transp. Syst.*, 2020.
- [26] S. Feng, Y. Feng, X. Yan, S. Shen, S. Xu, and H. X. Liu, "Safety assessment of highly automated driving systems in test tracks: A new framework," *Accid. Anal. Prev.*, vol. 144, p. 105664, 2020.
- [27] M. T. Horváth, Q. Lu, T. Tettamanti, Á. Török, and Z. Szalay, "Vehicle-In-The-Loop (VIL) and Scenario-In-The-Loop (SCIL) Automotive Simulation Concepts from the Perspectives of Traffic Simulation and Traffic Control," *Transp. Telecommun.*, vol. 20, no.

- 2, pp. 153–161, 2019.
- [28] D. J. Fremont *et al.*, “Formal Scenario-Based Testing of Autonomous Vehicles: From Simulation to the Real World.” 2020.
- [29] Z. Xu, M. Wang, F. Zhang, S. Jin, J. Zhang, and X. Zhao, “PaTAVTT: A hardware-in-the-loop scaled platform for testing autonomous vehicle trajectory tracking,” *J. Adv. Transp.*, vol. 2017, 2017.
- [30] N. Uchida, T. Tagawa, and K. Sato, “Development of an augmented reality vehicle for driver performance evaluation,” *IEEE Intell. Transp. Syst. Mag.*, vol. 9, no. 1, pp. 35–41, 2017.
- [31] L. Li *et al.*, “Parallel testing of vehicle intelligence via virtual-real interaction,” 2019.
- [32] Y. Feng, C. Yu, S. Xu, H. X. Liu, and H. Peng, “An augmented reality environment for connected and automated vehicle testing and evaluation,” in *2018 IEEE Intelligent Vehicles Symposium (IV)*, 2018, pp. 1549–1554.
- [33] J. Ma, F. Zhou, Z. Huang, C. L. Melson, R. James, and X. Zhang, “Hardware-in-the-loop testing of connected and automated vehicle applications: a use case for queue-aware signalized intersection approach and departure,” *Transp. Res. Rec.*, vol. 2672, no. 22, pp. 36–46, 2018.
- [34] T. Tettamanti, M. Szalai, S. Vass, and V. Tihanyi, “Vehicle-In-the-Loop Test Environment for Autonomous Driving with Microscopic Traffic Simulation,” *2018 IEEE Int. Conf. Veh. Electron. Safety, ICVES 2018*, 2018.
- [35] T. Nothdurft *et al.*, “Stadtpilot: First fully autonomous test drives in urban traffic,” *IEEE Conf. Intell. Transp. Syst. Proceedings, ITSC*, pp. 919–924, 2011.
- [36] A. Broggi *et al.*, “PROUD-Public Road Urban Driverless-Car Test,” *IEEE Trans. Intell. Transp. Syst.*, vol. 16, no. 6, pp. 3508–3519, 2015.
- [37] F. Kunz *et al.*, “Autonomous driving at Ulm University: A modular, robust, and sensor-independent fusion approach,” *IEEE Intell. Veh. Symp. Proc.*, vol. 2015-Augus, no. Iv, pp. 666–673, 2015.
- [38] A. Broggi *et al.*, “Extensive tests of autonomous driving technologies,” *IEEE Trans. Intell. Transp. Syst.*, vol. 14, no. 3, pp. 1403–1415, 2013.
- [39] J. Spears, J. Lutin, Y. Wang, R. Ke, and S. M. Clancy, “Active Safety-Collision Warning Pilot in Washington State,” 2017.
- [40] H. H. Soule *et al.*, “Testing an automated collision avoidance and emergency braking system for buses,” *Transp. Res. Rec.*, p. 0361198120912431, 2020.
- [41] C. D. Harper, C. T. Hendrickson, and C. Samaras, “Cost and benefit estimates of partially-automated vehicle collision avoidance technologies,” *Accid. Anal. Prev.*, vol. 95, pp. 104–115, 2016.
- [42] X. Zhao, Z. Wang, Z. Xu, Y. Wang, X. Li, and X. Qu, “Field experiments on longitudinal characteristics of human driver behavior following an autonomous vehicle,” *Transp. Res. Part C Emerg. Technol.*, vol. 114, no. February, pp. 205–224, 2020.
- [43] K. Raboy, J. Ma, E. Leslie, and F. Zhou, “A proof-of-concept field experiment on cooperative lane change maneuvers using a prototype connected automated vehicle testing platform,” *J. Intell. Transp. Syst.*, pp. 1–16, 2020.
- [44] A. Geiger, P. Lenz, C. Stiller, and R. Urtasun, “Vision meets robotics: The kitti dataset,” *Int. J. Rob. Res.*, vol. 32, no. 11, pp. 1231–1237, 2013.
- [45] Z. Kong, J. Guo, A. Li, and C. Liu, “PhysGAN: Generating Physical-World-Resilient Adversarial Examples for Autonomous Driving,” in *Proceedings of the IEEE/CVF Conference on Computer Vision and Pattern Recognition*, 2020, pp. 14254–14263.
- [46] E. de Gelder, J. P. Paardekooper, O. Op den Camp, and B. De Schutter, “Safety assessment of automated vehicles: how to determine whether we have collected enough field data?,” *Traffic Inj. Prev.*, vol. 20, no. sup1, pp. S162–S170, 2019.
- [47] M. Kilicarslan and J. Y. Zheng, “Predict Vehicle Collision by TTC from Motion Using a Single Video Camera,” *IEEE Trans. Intell. Transp. Syst.*, vol. 20, no. 2, pp. 522–533, 2019.
- [48] Y. Zhuang, R. Ke, and Y. Wang, “Edge-Based Traffic Flow Data Collection Method Using Onboard Monocular Camera,” *J. Transp. Eng. Part A Syst.*, vol. 146, no. 9, p. 4020096, 2020.
- [49] R. Ke, Z. Li, J. Tang, Z. Pan, and Y. Wang, “Real-time traffic flow parameter estimation from UAV video based on ensemble classifier and optical flow,” *IEEE Trans. Intell. Transp. Syst.*, no. 99, pp. 1–11, 2018.
- [50] R. Ke, Y. Zhuang, Z. Pu, and Y. Wang, “A Smart, Efficient, and Reliable Parking Surveillance System with Edge Artificial Intelligence on IoT Devices,” *IEEE Trans. Intell. Transp. Syst.*, 2020.
- [51] R. Ke, S. Feng, Z. Cui, and Y. Wang, “Advanced framework for microscopic and lane-level macroscopic traffic parameters estimation from UAV video,” *IET Intell. Transp. Syst.*, 2020.
- [52] E. Dagan, O. Mano, G. P. Stein, and A. Shashua, “Forward collision warning with a single camera,” *IEEE Intell. Veh. Symp. Proc.*, pp. 37–42, 2004.
- [53] M. Naphade *et al.*, “The 4th AI City Challenge.” 2020.